On-line RPLC x SFC hyphenated to high resolution mass spectrometry for the characterization of third generation bio-oils

Jason Devaux, Mélanie Mignot, Florent Rouvière, Isabelle François, Carlos Afonso, Sabine Heinisch

On-line reversed-phase liquid chromatography x supercritical fluid chromatography coupled to high-resolution mass spectrometry: a powerful tool for the characterization of advanced biofuels

Jason Devaux[1, 2, 3], Mélanie Mignot[2, 3], Florent Rouvière[1], Isabelle François[4], Carlos Afonso[2, 3], Sabine Heinisch[1*]

[1] Université de Lyon, Institut des Sciences Analytiques, UMR 5280 CNRS, 5 rue de la Doua, 69100 Villeurbanne, France

[2] COBRA, Normandie Université, Université de Rouen, INSA de Rouen, CNRS, UMR 6014, IRCOF 1 rue Tesnière, Mont Saint Aignan 76821, France

[3] International Joint Laboratory – iC2MC: Complex Matrices Molecular Characterization, TRTG, BP 27, 76700 Harfleur, France

[4] Chromisa Scientific, Schoolstraat 3, 9520 Sint-Lievens-Houtem, Belgium

* Corresponding author: E-mail sabine.heinisch@univ-lyon1.fr

Abstract

Bio-oils obtained by thermochemical or biochemical conversion of biomass represent a promising source of energy to complement fossil fuels, in particular for maritime or air transport for which the use of hydrogen or electricity appears complicated. As these bio-oils are very rich in water and heteroatoms, additional treatments are necessary before they can be used as biofuel. In order to improve the efficiency of these treatments, it is important to have a thorough knowledge of the composition of the bio-oil. The characterization of bio-oils is difficult because they are very complex mixtures with thousands of compounds covering a very wide range of molecular weight and polarity. Due to the high degree of orthogonality between the two chromatographic dimensions, the on-line combination of reversed-phase liquid chromatography and supercritical fluid chromatography (on-line RPLC x SFC) can significantly improve the characterization of such complex matrices. The hyphenation was optimized by selecting, in SFC, the stationary phase, the co-solvent, the make-up solvent prior to high resolution mass spectrometry (HRMS), and the injection solvent. Additionally, a new interface configuration is described. Quality descriptors such as the occupation of the separation space, the peak shapes and the signal intensity were considered to determine the optimal conditions. The best results were obtained with bare silica, a co-solvent composed of acetonitrile and methanol (50/50, v/v), a make-up solvent composed of methanol (90%) and water (10%) with formic acid (0.1%), an addition of co-solvent through an

additional pump for SFC separation in a 2.1 mm column, and an hydro-organic solvent as injection solvent. The optimized setup was used to analyse two microalgae bio-oils: the full bio-oil coming from hydrothermal liquefaction and Soxhlet extraction of microalgae, and the gasoline cut obtained after distillation of the full bio-oil. Results in on-line RPLC x SFC-qTOF were particularly interesting, with very good peak shapes and high reproducibility. Moreover, the high degree of orthogonality for microalgae bio-oils of RPLC and SFC was highlighted by the very large occupation of the separation space. Isomeric profiles of compound families could be obtained in RPLC x SFC-qTOF and many isomers not separated in SFC alone were separated in RPLC and vice versa, thus showing the complementarity of the two chromatographic techniques.

Keywords

On-line RPLC x SFC, Comprehensive two-dimensional chromatography, advanced biofuels, microalgae bio-oil, HRMS

1. Introduction

With the depletion of fossil fuels and the increasing global energy demand, the development of sustainable energy sources is of paramount importance. Microalgal biomass is a promising resource to produce biofuels and value-added products because of its high photosynthetic efficiency and fast growth rate. Moreover, microalgae only need water, light, nutrients, and carbon to grow [1,2]. Microalgae can then be converted into bio-oils by thermochemical processes. Although some studies used pyrolysis to convert the microalgae [3–5], they are converted most often by hydrothermal liquefaction [6–9] in order to avoid the drying step of the raw material and thus additional costs [10,11]. The main components of microalgae include proteins, carbohydrates, and lipids. During the thermochemical conversion, they are transformed into smaller oxygenated and nitrogenous molecules [12]. The high levels of water and heteroatomic compounds make the bio-oils chemically unstable and corrosive. Upgrading treatments are therefore necessary to reduce the heteroatomic content and increase the calorific value of the bio-oils before use [13,14]. To optimize these treatments, a deep understanding of bio-oils composition is required. However, their characterization is a challenging task as those are complex mixtures including thousands of compounds covering a wide range of molecular weight and polarity. Most of the time complex mixtures are analyzed by direct introduction (DI) into a Fourier transform ion cyclotron resonance mass spectrometer (FTICR-MS) [15,16], allowing the assignment of a molecular formula to thousands of *m/z* ratios with a high level of confidence. However, two issues arise with direct introduction: (1) the impossibility to differentiate the numerous isomers present in bio-oil samples and (2) the possible matrix effects that prevent the detection of some compounds due to ion suppression in the ionization source.

To overcome these issues, chromatography is often hyphenated to mass spectrometry. Gas chromatography (GC) has been used to separate bio-oils from lignocellulosic biomass [17,18]. However, GC is limited to volatile and high-temperature stable compounds. As a result, many compounds cannot be analysed by GC unless a derivatization step is carried out. Liquid chromatography (LC) and supercritical fluid chromatography (SFC) are promising techniques to separate polar and neutral compounds. Crepier et al. [19] used SFC hyphenated to an ion trap time-of-flight mass spectrometer with an atmospheric pressure chemical ionization source in

negative mode (APCI(−)-IT-TOF) for the characterization of fast pyrolysis bio-oil from conifer sawdust, and they compared the results obtained with DI-APCI(−)-FTICR. The interest of SFC for isomer separation was demonstrated for several molecular formulae, with sometimes more than three peaks observed at different retention times. Moreover, although the number of assigned molecular formulae was lower in SFC-HRMS (1379 vs. 3949 in DI-FTICR), differences in the oxygen distribution were highlighted. The most intense compounds in SFC-HRMS were less oxygenated compared to DI-FTICR, suggesting that the matrix impacted the ionization of some compounds [19].

For complex mixtures, comprehensive two-dimensional liquid chromatography (LC x LC) is a technique of choice, leading to an impressive separation power when the separation mechanisms are different. Although the mechanisms are similar using two reversed-phase liquid chromatography systems (RPLC x RPLC), on-line RPLC x RPLC was found to be very attractive for ionizable compounds (peptides or pharmaceuticals) by just changing the mobile phase pH and possibly the stationary phase between the two dimensions [20]. As bio-oil compounds are essentially neutral, RPLC x RPLC is much less attractive, the stationary phase change alone being usually insufficient. However, RPLC x RPLC was applied to the analysis of the aqueous phase of lignocellulosic biomass pyrolysis bio-oil. A porous graphitic carbon column and a bonded silica-based column were used in first (^{1}D) and second (^{2}D) dimension respectively, leading to a fairly good occupation of the retention space [21]. Two different bonded silica-based columns were also used [22,23], but despite different stationary and mobile phases, the retention mechanisms were related, leading to peaks distributed along the 2D-separation space diagonal and hence to a low retention space coverage. The occupation of the retention space is a key parameter and the combination of RPLC and SFC is a much more promising technique for neutral compounds. Off-line RPLC x SFC has been applied to pharmaceuticals [24], natural products such as Chinese plants [25,26], and fragrant oil [27]. The two main advantages of the off-line approach are (i) the possibility to treat the collected fraction and hence to avoid detrimental injection effects arising from the injection of large hydro-organic solvent volumes in SFC and (ii) the possibility to optimize the two dimensions separately, therefore, the performance in off-line mode is expected to be higher but at the cost of a longer analysis time. However, the off-line approach has many drawbacks that do not exist with the on-line one: (i) the fractions are diluted during the fraction collection, (ii) some compounds may be lost during the fraction treatment, (iii) contamination can occur all along the process and (iv) data processing is not straightforward at all. On-line SFC x RPLC was first set up by François et al. [28,29] but due to the nature of the first dimension mobile phase, the authors had to use two two-positions/ten-port switching valve with two loops packed with octadecyl (C_{18}) silica to avoid signal interferences due to the decompressed CO_2 which became apparent in the UV trace. The packed loops allowed CO_2 depressurization and the trapping of the analytes before their injection into the RPLC system by adding water after the backpressure regulator (BPR) to enhance focusing. The water was also used to serve solvent displacement and hence efficiently remove the residual CO_2 gas prior to introduction of the fractions in the ^{2}D. In contrast, in RPLC x SFC, since the first dimension eluent is liquid, a conventional LC x LC valve with two empty loops can be used. Sarrut et al. compared on-line RPLC x RPLC with a Hypercarb column in ^{1}D and RPLC x SFC for the analysis of an aqueous phase of lignocellulosic bio-oil [30]. They showed that the degree of orthogonality was much higher in RPLC x SFC, leading to a small increase in peak capacity.

The objective of this work was to demonstrate the benefits of on-line RPLC x SFC hyphenated to a quadrupole time-of-flight (qTOF) mass spectrometer for the characterization of microalgae

based bio-oils. Key parameters were optimized for this analytical technique. Those parameters included the stationary and mobile phases in SFC, the make-up solvent prior to the qTOF mass spectrometer and the interface between the two dimensions of separation. An illustrative application is given by comparing two different samples coming from two different stages of the conversion process.

2. Material and methods

2.1. Chemicals and sample preparation

Acetonitrile (ACN), methanol (MeOH), and formic acid (LC-MS grade) were purchased from Sigma-Aldrich (Steinheim, Germany). HPLC grade toluene was from Biosolve Chimie (Dieuze, France). Water was provided by an Elga Purelab Classic UV purification system (Veolia water STI, Le Plessis Robinson, France). High purity CO_2 (99.99%) was obtained from Air Liquide (Paris, France)

Two bio-oil samples coming from the VASCO2 project were supplied by TotalEnergies TRTG (Total Research and Technology Gonfreville). The first sample was a bio-oil obtained by hydrothermal liquefaction of a wild microalgae consortia and the second one was the gasoline cut of the full bio-oil after distillation. A detailed description of bio-oil production was made by Barrère-Mangote et al. [31]. The full bio-oil and the gasoline cut were first dissolved in toluene at 22 mg/mL and in methanol at 178 mg/mL respectively. Stock solutions were further diluted at 5 mg/mL for the full bio-oil and 16 mg/mL for the gasoline cut in methanol and filtered through PVDF membrane (0.22 µm) before injection.

2.2. Columns

RPLC separations were carried out using a XBridge BEH C_{18} column (50x1.0 mm; 3.5 µm) and three columns were evaluated for the unidimensional SFC separation: Viridis BEH 2-EP (100x3.0 mm; 1.7 µm), Viridis BEH (100x3.0 mm; 1.7 µm), and Torus 2-PIC (50x3.0 mm; 1.7 µm) all from Waters. For on-line RPLC x SFC analyses, an additional column from Waters was used in the second dimension: Acquity BEH HILIC (50x2.1 mm; 1.7 µm).

2.3 Instruments and chromatographic methods:

2.3.1. 1D-SFC

SFC separations were carried out using a Waters UPC² (Milford, MA, USA) equipped with a binary solvent delivery pump, an autosampler with a 10 µL loop, an isocratic pump for the make-up solvent, a column oven compatible with temperatures up to 90°C, a diode array detector (DAD) with a 8.4 µL flow-cell and a backpressure regulator (BPR). The dwell volume was 250 µL, it was measured according to the procedure described by Sarrut et al. [30]. Three different columns, all from Waters were assessed: Viridis BEH 2-EP (100x3.0 mm; 1.7 µm), Viridis BEH (100x3.0 mm; 1.7 µm), and Torus 2-PIC (50x3.0 mm; 1.7 µm) and three solvents B were compared: methanol, acetonitrile/water (98/2, v/v), and methanol/acetonitrile (50/50, v/v). The gradient times were adapted to the column dead times (t_0): 1%B for $4t_0$, 1-60%B in $59t_0$ with acetonitrile/water or 1-

40%B in 40t_0 with methanol and methanol/acetonitrile. For all experiments, the injected volume, the flow rate, the oven temperature, and the BPR pressure were set at 1 µL, 1400 µL/min, 30°C, and 137 bar respectively. The DAD outlet was connected to the mass spectrometer via a double T-union allowing pressure regulation and the addition of a make-up solvent with a flow rate of 500 µL/min. The instrument was controlled using Empower software from Waters.

2.3.2. On-line RPLC x SFC

RPLC analyses were carried out using the first dimension of a 2D I-Class system from Waters (Milford, MA, USA) equipped with a binary solvent delivery pump, an autosampler with a 20 µL flow-through needle, two column ovens with a maximum temperature of 90°C, a DAD equipped with a 0.5 µL cell. The Dwell volume was 110 µL. The 2D I-Class and the UPC² were connected via a 10-port/2-positions valve equipped with two identical loops (geometrically estimated volume of 6 µL). Two valve configurations were compared, the standard (Fig. 1a) and the new (Fig. 1b) one. This latter was selected for the bio-oil analyses as discussed in section 4. Both dimensions were controlled using Empower 3 and were synchronized thanks to external events. On-line RPLC x SFC conditions are given in Table 1.

2.4. Mass spectrometry parameters

Mass spectra were acquired using an Agilent 6560 IM-qTOF from Agilent Technologies (Waldbronn, Germany) equipped with a JetStream electrospray ionization (ESI) source in positive mode. Data acquisition was performed using MassHunter software from Agilent Technologies over the *m/z* 90-900 with an acquisition rate of 5 Hz. The ionization parameters were set as follows: drying gas temperature, 300°C; drying gas flow rate, 11 L/min; sheath gas temperature, 350°C; sheath gas flow rate, 11 L/min; nebulizer pressure, 40 psi; fragmentor, 185 V and capillary voltage, 3500 V. After acquisition, data were sent to an Excel sheet and rearranged in 2D-contour plots using an in-house program developed with Matlab (V7.12.0635).

3. Calculations

The mobile phase composition at elution was calculated according to:

$$Ce = C_i + \frac{C_f - C_i}{t_g} \times (t_r - t_0 - t_d - t_{iso}) \quad (1)$$

With C_i and C_f being the initial and final gradient composition and t_r, t_g, t_0, t_d, and t_{iso} being the solute retention time, the gradient time, the column dead time, the instrument dwell time, and the duration of the initial isocratic hold respectively.

The peak capacity for 1D separations is given by:

$$n_{1D} = 1 + \frac{t_n - t_1}{w} \quad (2)$$

with t_n and t_1 corresponding to the retention time of the most and the least retained peak respectively and w to the average 4σ peak width.

In RPLC x SFC, the effective peak capacity can be calculated according to [32]:

$$n_{RPLC \times SFC} = n_{RPLC} \times \alpha \times (1 - \gamma) + \mathrm{n_{RPLC}} \times \mathrm{n_{SFC}} \times \alpha\gamma \quad (3)$$

where γ is the fraction of the separation space occupied by the peaks and α is the undersampling correction factor. γ is calculated according to the procedure described by D'Attoma et al. [32].

$$\alpha = \frac{1}{\sqrt{1+0.21\times(\frac{4t_s}{w})^2}} \quad (4)$$

With t_s being the sampling time.

The injection volume in the second dimension is given by:

$${}^2V_i = t_s \times {}^1F \quad (5)$$

With ^{1}F being the flow rate of the first dimension.

4. Results and discussion

4.1. 1D-SFC method development

4.1.1. Stationary and mobile phases

Three different stationary phases were assessed in 1D-SFC for the separation of a gasoline cut. Those include: Viridis BEH 2-EP, Viridis BEH, and Torus 2-PIC. The three corresponding base peak chromatograms (BPC) (MeOH as co-solvent) are presented in Fig. 2. Viridis BEH 2-EP and Torus 2-PIC show similar space coverage with a composition range from 1%B to 15%B and 1%B to 16%B respectively (Eq. 1). The composition range with Viridis BEH was almost twice as wide (27%) suggesting that this stationary phase was more suitable for this study. The peak capacity was calculated for the three columns using Eq. 2, because the column lengths were different, peak capacities were normalized to a 10cm-length. It represents the number of peaks that can theoretically be separated side by side with a resolution of 1, which makes it a reliable descriptor of the separation power. Due to the complexity of the sample, leading to a large number of coelutions, the peak capacities were calculated using the same eight extracted ion chromatograms (EICs). The 4σ peak width values and the resulting peak capacities are listed in Table S1. The peak capacity was more than twice as high (i.e. 185) using the Viridis BEH column than with the other two columns (about 80). It is important to note that peak widths with MS detection are much larger than with UV detection due to additional peak broadening (tubing, introduction capillary, source, CO_2 depressurization [33]…), resulting in lower peak capacities than those that could be expected. Given these results, the Viridis BEH column was selected in SFC for the rest of the study.

Co-solvents are used to increase the polarity of CO_2-based mobile phase and to modify the stationary phase (by adsorption onto its surface). Their concentration in the mobile phase impacts the critical point (pressure and temperature above which the mixture is in a supercritical state) and the density of the mobile phase. Co-solvents also affect sample solubility, eluent strength and selectivity [34]. Three co-solvents were investigated including methanol, a mixture of acetonitrile and water (98/2, v/v), and a mixture of methanol and acetonitrile (50/50, v/v). BPCs for the separation of the gasoline cut are presented in Fig. S1. The selected criterion values are listed in Table 2. As it can be shown, the peak capacity is similar for the three co-solvents (about 190), with a larger occupation of the retention space using the mixture of acetonitrile and water. This is related to the lower eluent strength of this co-solvent compared to the other two. While the large

composition range can be attractive for one-dimensional separations, it is much less so for the second dimension of on-line comprehensive 2D-LC, which must be rapid while maintaining a sufficiently high peak capacity. The upper pressure is also important for selecting the co-solvent. With the same flow rate of 1.4 mL/min, the upper pressure was slightly lower (Table 2) with the mixture of methanol and acetonitrile (50/50), which allowed us to increase the flow rate and hence to decrease the normalized gradient slope. Considering the above, our selected SFC system consisted of a Viridis BEH column and a mixture of methanol and acetonitrile (50/50, v/v) as co-solvent.

4.1.2. SFC make-up optimization

In SFC-MS the addition of a make-up solvent is often recommended to avoid solute precipitation when CO_2 depressurization occurs, especially at the beginning of the gradient elution. Since this solvent is supplied by an additional pump, it can be individually optimized to improve the ionization yield without affecting the chromatographic separation. Plachká et al. showed that the addition of water in the make-up solvent could increase the MS response up to 50% [35]. Thus, the gasoline cut was injected under the above selected conditions by varying the percentage of water (0 to 30%) in the make-up solvent composed of MeOH, 0.1% formic acid and water. The results are presented in Fig. 3a. For easier interpretation, 5 EICs (*m/z* 223.181, 270.280, 278.248, 284.295 and 317.102) were chosen along the chromatogram as representative compounds. For all the observed peaks, the intensity increased sharply (by a factor of up to 5) by adding 10% of water, which could be explained by the acidic properties of the SFC mobile phase and make-up. Indeed, CO_2 reacts with MeOH and water to form methoxylcarbonic acid and carbonic acid respectively. The apparent pH is therefore acidic and the MS response is increased in ESI(+) [35,36]. For microalgae bio-oils, this increase is significant due to the high proportion of nitrogenous compounds. The greater the amount of water, the higher the signal is obtained. However, as illustrated in Fig. 3b, the intensity seems to reach a plateau at high water percentage. Indeed, when the mixture entering the ionization source is too rich in water, the solvent desolvation is more difficult and the signal intensity no longer increases but may even decrease. This phenomenon and the variation in signal intensity were found to be compound-dependent as illustrated by the curves in Fig.3b. For the compound represented by the blue square, the curve increases sharply from 0 to 10% but is constant thereafter. The trend is different for the compound eluted at 2.641 min (green triangles), the increase in intensity from 10 to 30% is significant, suggesting that the plateau has not yet been reached. Although the highest intensity could be obtained with 30%H_2O or more, the RPLC x SFC analyses were performed with 10%H_2O for several reasons: (i) at 30%H_2O, the water amount is too high and phase separation can occur between the gaseous and the liquid phase, leading to a heterogeneous fluid and pressure instability. (ii) the increase in intensity being compound-dependent, a further increase in the water content could have led to too high signal for the compounds that responded the most and therefore to a too wide dynamic range.

4.2. On-line RPLC x SFC

4.2.1. Interface development

In comprehensive 2D-LC, although easier to implement, the off-line mode has major drawbacks compared to the on-line mode. Those include (i) additional dilution during fraction collection, (ii)

possible loss of compounds or contamination during fraction treatment, and (iii) time-consuming data processing. We therefore opted for the on-line mode that has become usual in LC x LC but is much less straightforward to implement in LC x SFC. First, unlike on-line LC x LC, there is no commercial instrument in LC x SFC. The two devices have to be hyphenated using a home-built interface design. The current research uses a via a 10-port/2-positions valve equipped with two identical loops. Second, flow splitting after LC and before the valve cannot be applied due to CO_2 depressurization. Third, for the same reason, the loops have to be completely filled which is not the case in LC x LC. Additionally, due to the absence of commercially available instrumentation and software, the operator needs to take care of data acquisition and data interpretation.

With a view to limit detrimental injection effects while injecting larger volumes in the SFC second dimension, we studied a new configuration for the interface (Fig. 1b) that we compared to the conventional one (Fig. 1a). With the conventional interface configuration, the two components of the mobile phase are mixed by the mixer device of the SFC instrument. The loop is thus flushed by the mobile phase (co-solvent and CO_2). With the new configuration, the co-solvent is supplied after the valve via a tee-union. The loop content is therefore flushed with CO_2 only. To compare the performance of the two interface configurations, the LC mobile phase was replaced by a mixture of acetonitrile and water (50/50) spiked with 50 ppm of caffeine, and the LC column was replaced by a zero dead volume union. The LC flow rate and the sampling time were set at 10 µL/min and 1.2 min respectively. With sample loops of 6 µL, 6 µL of the mixture was expected to be injected in SFC. The obtained caffeine peaks using the classical valve configuration are presented in Fig. 4a and c, it is clearly noticeable that the peaks are large and distorted in this case. However, with the second configuration (Fig. 4b and d) the peak shapes are clearly improved, leading to thinner peaks and therefore to a higher peak capacity. With the conventional configuration and partial loop mode, droplets of co-solvent cover the walls of the loop during valve switching due to CO_2 depressurization [30]. Using this new configuration, the effluent is composed of pure CO_2. The fraction coming from the first dimension enters a loop completely empty of liquid and co-solvent droplets cannot exist, suggesting that a partial loop injection becomes possible. This new interface configuration was therefore chosen for our on-line RPLC x SFC analyses.

4.2.2. Injection effects in ^{2}D-SFC

In SFC, severe injection issues can occur with too large injection volumes, especially with solvents that contain water [37,38]. In comprehensive LC x LC, the injected volume in the second dimension depends on both the first dimension flow rate and the sampling time (Eq. 5). Due to the nature of the SFC mobile phase, the flow cannot be split before the valve without depressurizing CO_2. The first dimension flow rate was therefore reduced to the minimum possible according to the gradient system used (i.e. 10 µL/min). With a sampling time of 0.6 min and a sample loop of 6 µL, the injection volume was therefore expected to be 6 µL. Injection effects in on-line LC x SFC were studied following the same approach as previously for the interface study. Two different column internal diameters (3.0 and 2.1 mm) were considered. The resulting peaks of caffeine are shown in Fig. 5. Surprisingly, the peak shapes are as good with 2.1 mm (Fig. 5a) as with 3.0 mm (Fig. 5b) i.d., the obtained peak widths being quite similar with ACN/water (50/50, v/v) as injection solvent. Based on these results, the 2.1 mm i.d. column was preferred because (i) sensitivity is expected to be higher for a given injection volume and (ii) the normalized gradient slope is lower for a given gradient time thus, increasing the peak capacity. The composition of the injection solvent was also studied since it has often been reported as a critical factor [39,40]. Fig. 5 c) shows the caffeine peaks obtained with three ACN/water (v/v) compositions (10/90, 50/50

and 90/10) and the 2.1 mm i.d. column. It was once again surprising to see that the injection solvent seemed to have no significant effects on both the peak shapes and the peak widths. The average peak width was about 0.47 s, leading to a peak capacity of about 20. These results showed that despite a high volume (6 µL) injected in different hydro-organic solvents, the caffeine peak kept a good shape, suggesting that the on-line RPLC x SFC coupling could provide promising results under such injection conditions. It should be underlined that such a result is in disagreement with studies highlighting the detrimental effect of hydro-organic solvents on peak shapes [38], but it should also be noted that this latter study is undertaken using traditional injection techniques and hence a mixed flow of CO_2 and co-solvent is passing through the injection loop at the time of injection. Therefore, the fact that sharp peak shapes are obtained in RPLC x SFC should be ascribed to the performance of the new interface configuration and the fact that the loop is flushed with CO_2, reducing diffusion in the tubing.

When using CO_2 only for the transfer and hence the injection of the fraction onto the SFC dimension, immiscibility undeniably occurs, certainly when the transfer solvent contains high concentrations of water. The extremely sharp peak shapes in the SFC dimension when injecting relatively large volumes of "strong" solvent might therefore be explained as a positive effect of that immiscibility. Similar behaviour has been observed by François et al. [41] when combining NPLC and RPLC in an on-line comprehensive setup. The authors carried out a gradient of 90/10 *n*-hexane/ethylacetate to 34/66 *n*-hexane/ethylacetate in the NPLC ^{1}D separation. Compounds present in fractions eluting at the end of the ^{1}D gradient (hence containing higher ethylacetate content) showed severe peak distortion in the ^{2}D RPLC separation, when the ^{2}D gradient was started using 40/60 H_2O/ACN. While *n*-hexane is immiscible in both H_2O as well as in ACN, ethylacetate is miscible in ACN, but not in H_2O. When starting the ^{2}D gradient with 100% H_2O, and hence creating full immiscibility of the fraction solvent at the start of the ^{2}D gradient, significant peak sharpening was observed.

As the injection of larger volumes of sample dissolved in relatively polar solvent is problematic in regular SFC analyses, the application of a similar injection approach as applied in the current RPLC x SFC interface could be considered advantageous as well.

4.2.3. Full bio-oil in on-line RPLC x SFC

The conditions in on-line RPLC x SFC, selected according to the above study, are listed in Table 1. Due to connection issues between the two instruments, it was impossible to apply a gradient time higher than 0.25 min with a sampling time of 0.6 min. The final composition in the SFC dimension was therefore set at 30%B so that the flow rate could be raised and the the normalized gradient slope reduced as much as possible (here 5.8%). The linear retention model is widely used in HPLC, especially in RPLC. It was recently found that it could be applied in SFC for bio-oil compounds [42]. The coefficients ($\log k_0$ and S) are usually calculated according to the linear solvent strength (LSS) theory from two preliminary runs. These coefficients were calculated for nine compounds by Osiris software (Euradif, France) from the retention data obtained with two normalized gradient slopes (i.e. 0.5 and 1.5%). Two different co-solvents (ACN/H_2O 98/2, v/v and ACN/MeOH 50/50, v/v) were considered for these calculations. Predicted retention times with extrapolated normalized gradient slopes (i.e. 3 and 5%) were found to be close enough to experimental retention times (errors of less than 5% and 10% with normalized gradient slopes of 3% and 5% respectively), thus validating the LSS model in the studied range. Fig. S2 shows the resulting variation of S with $\log k_0$. As can be observed, for both co-solvents, S decreases as the retention increases ($\log k_0$ increases). The S values become very low with the ACN/H_2O co-solvent

for the most retained compounds, theoretically indicating that the final gradient composition must be very high to elute them unless using a very low normalized gradient slope, which is impossible in the second dimension. The ACN/MeOH co-solvent was therefore found to be more appropriate in on-line RPLC x SFC. However, even with this co-solvent and due to the reduction of S with the retention, some highly retained compounds could not be eluted under RPLC x SFC conditions as highlighted in Fig. S3, showing the same 3 EICs in 1D-SFC (normalized gradient slope of 1%) and in on-line RPLC x SFC (normalized gradient slope of 5.8%).

The contour plot obtained for 44 EICs from the full bio-oil is presented in Fig. 6a. The complementarity of the two techniques is clearly demonstrated as several compounds not separated in RPLC alone appear separated in SFC and conversely. The peaks are well distributed over the separation space, leading to a distribution across the retention space close to 100% and a calculated effective peak capacity of about 700 (Eq. 3, 4 and Table S2). The SFC chromatograms of three successive injections are presented in Fig. 6b. The obtained excellent peak shapes are in accordance with the observations made in section 4.2.2 for caffeine, although, in both cases, the injection conditions were unfavourable. Moreover, the SFC retention times proved to be highly repeatable between several consecutive injections as illustrated by the vertical dashed lines. Isomeric separations in both dimensions are illustrated in Fig. 7 by three extracted ion chromatograms (EICs with *m/z* 242.248, 277.216 and 284.295). The high separation power enabled to separate the different compounds in both RPLC and SFC. RPLC mainly separates compounds according to their *m/z* ratios but also a few isomers such as EIC 277.216. The two spots at approximately 33 and 35 minutes are separated in RPLC only. SFC well separates the isomers. This is clearly demonstrated with EIC 284.295 as three spots well separated in SFC, are coeluted in RPLC. Finally, for the three considered EICs, five peaks were separated in RPLC and four in SFC, leading to 8 well separated spots in on-line RPLC x SFC, showing the great interest of using these two dimensions simultaneously.

4.2.4. 1D-SFC vs. on-line RPLC x SFC

One of the many compelling examples of the value of on-line RPLC x SFC over 1D-SFC is shown in Fig. 8 with the comparison of the separations (EIC 172.170 and BPC) between 1D-SFC-HRMS (Fig. 8a) and on-line RPLC x SFC-HRMS (Fig. 8b). The peak intensity for the EIC 172.170 is much higher in on-line RPLC x SFC compared to 1D-SFC (up to 10 times higher) while the quantity injected was only 3 times higher. This large difference can probably be attributed to the upstream RPLC separation. In 1D-SFC, the peaks of EIC 172.170 are coeluted with several other compounds as illustrated by the overlapped chromatograms in Fig. 8a (EIC in red and BPC in black). In on-line RPLC x SFC (Fig. 8b), the RPLC separation allows to separate the red peaks from the main peaks of the matrix, resulting in less ionization competition and an increased sensitivity.

4.3. Comparison of two bio-oil samples

Two microalgae bio-oil samples were analyzed in on-line RPLC x SFC-qTOF. The full bio-oil (sample #1) was obtained after hydrothermal liquefaction and Soxhlet extraction. The gasoline cut (sample #2) was obtained after distillation of the full bio-oil. The two samples were therefore related and thus, expected to have many compounds in common. The contour plots (BPCs) are presented in Fig. 9a for sample #1 and 9b for sample #2. As expected, the separations are very similar for both samples. The most intense compounds are strongly retained in RPLC (elution between 40 and 55 minutes). Some differences can nevertheless be observed between the two

BPCs, especially in the dashed black squares, showing the presence of many spots in Fig. 9a that do not exist in Fig. 9b. This suggests that several compounds were removed or converted during the additional processing step (i.e. distillation). This is also illustrated in Figs. 9c and 9d that show the EICs (*m/z* 200.201) for sample #1 and #2 respectively. Two spots can be observed in Fig. 9d while three spots in Fig. 9c, the additional spot being circled in red. Considering the distribution of the spots in the two contour plots, this additional compound (at 16 s in SFC and 33 min in RPLC) would have been eluted with another one in both 1D-SFC and 1D-RPLC, thus showing the interest of using both techniques simultaneously.

5. Conclusions

The characterization of microalgae bio-oils is difficult because these are very complex mixtures with thousands of compounds covering a very wide range of polarity and molecular weight. Two microalgae bio-oils were analysed for the first time in on-line RPLC x SFC-qTOF to illustrate the potential of this technique for such complex matrices. These included a full bio-oil coming from hydrothermal liquefaction and Soxhlet extraction of microalgae, and the gasoline cut obtained after distillation of the full bio-oil. Considering quality descriptors such as peak capacity, peak shape, and peak intensity, key parameters were optimized in 1D-SFC and then in on-line RPLC x SFC.

The best results in 1D-SFC were obtained with bare silica as stationary phase, acetonitrile/methanol (50/50, v/v) as co-solvent, and a make-up solvent composed of methanol (90%), water (10%) and formic acid (0.1%).

In on-line RPLC x SFC, the peak capacity was found to be similar, for the same injection column between 3.0 and 2.1 mm i.d. columns. Consequently, the 2.1 mm i.d. column was selected, which increased the sensitivity while improving the peak capacity by decreasing the normalized gradient slope. Injection solvent effects were also assessed by injecting caffeine in various hydro-organic solvents, under on-line RPLC x SFC conditions. Interestingly, acetonitrile/water solvents with up to 90% water still provided good peak shapes. Such good results could be ascribed to a new interface configuration, with the co-solvent supplied directly after the valve. It is suggested in this study that creating full immiscibility between CO_2 and the injection solvent at the beginning of the ^{2}D gradient could make the peaks more focused.

The large retention space coverage provided by the two orthogonal dimensions and the resulting high separation power allowed us to discriminate the two samples studied despite their high degree of similarity. Very good time repeatability was shown between the analyses of successive fractions in the second dimension, demonstrating the reliability of our on-line RPLC x SFC setup. However, incomplete elution in SFC of the most retained compounds was reported due to the current limitations of the equipment used.

Isomeric profiles of compound families could be obtained in RPLC x SFC-qTOF. Many isomers that could not be separated in SFC alone could be in RPLC and vice versa, showing the great complementarity of the two chromatographic techniques.

CRediT authorship contribution statement

Jason Devaux: Conceptualization, Investigation, Formal analysis, Writing – original draft. **Mélanie Mignot**: Resources, Funding acquisition, Supervision, Writing – review & editing. **Florent Rouvière**: Investigation, validation. **Isabelle François**: Conceptualization, Writing – review & editing**. Carlos Afonso**: Supervision, Resources, Writing – review & editing. **Sabine Heinisch**: Methodology, Formal analysis, Conceptualization, Resources, Supervision, Writing – review & editing.

Declaration of Competing Interest

The authors declare that they have no known competing financial interests or personal relationships that could have appeared to influence the work reported in this paper.

Acknowledgements

The authors would like to thank TotalEnergies TRTG, CEA LITEN Grenoble and COLDEP for giving the two bio-oil samples coming from the VASCO2 project. This work has been partially supported by University of Rouen Normandy, INSA Rouen Normandy, Institute of Analytical Science (Labex iMust, University of Lyon) the Centre National de la Recherche Scientifique (CNRS), European Regional Development Fund (ERDF) Nº HN0001343, Labex SynOrg (ANR-11-LABX-0029) for financing Jason Devaux's PhD, Carnot Institute I2C, the graduate school for research XL-Chem (ANR-18-EURE-0020 XL CHEM), Region Normandie.

Figure caption

Fig. 1: Schematic representation of the on-line RPLC x SFC setup. (a) standard configuration and (b) new configuration.

Fig. 2: 1D-SFC separation of gasoline cut with three different columns: (a) Viridis BEH, (b) Torus 2-PIC and (c) Viridis BEH 2-EP. The dashed blue lines correspond to gradient profiles at elution. Analytical conditions in section 2.3.1.

Fig. 3: Effect of the addition of water in the make-up solvent. (a) Sum of 5 EICs (m/z 223.181, 270.280, 278.248, 284.295, and 317.102) with different amount of water in the make-up solvent. (b) Peak intensity (retention times of 1.536, 2.246 and 2.641 min in Fig.3 (a) versus percentage of water in the make-up solvent.

Fig. 4: Three successive separations of caffeine in on-line LC x SFC with (a) the standard configuration and (b) the new configuration. Corresponding contour plots with (c) the standard configuration and (d) the new configuration. The two configurations are shown in Fig. 1. ^{1}D conditions: no column, isocratic infusion of caffeine (50 ppm in acetonitrile/water 50/50) at 10 µL/min, T = 30°C. ^{2}D conditions: BEH HILIC (50x2.1 mm; 1.7 µm) at 1.8 mL/min, 30°C., P_{BPR} = 150 bar, gradient from 5% to 30%ACN/MeOH (50/50) in 0.25 min, t_s = 1.2 min, 6 µL injected, make-up solvent: MeOH/H_2O (90/10) + 0.1%FA.

Fig. 5: Illustration of injection solvent effects in ^{2}D-SFC under on-line LC x SFC conditions. Two successive separations of caffeine in SFC with two column internal diameters: (a) 2.1 mm and (b)

3.0 mm. (c) Effect of the injection solvent on a 2.1 mm i.d. column, ^{1}D conditions: no column, solution of caffeine (50 ppm in acetonitrile/water 50/50) at 10 µL/min, 30°C, sampling time: 0.6 min. ^{2}D conditions: Acquity BEH HILIC (50x2.1 mm; 1.7 µm), P_{BPR}: 150 bar, A: CO_2, B: ACN/MeOH (50/50), 5% to 30%B in 0.25 min, 1.8 mL/min, 6 µL injected, make-up solvent: MeOH/H_2O (90/10) + 0.1%FA.

Fig. 6: (a) On-line RPLC x SFC separation of the full bio-oil sample: contour plot representing the sum of 44 EICs (b) ^{2}D separation of three successive fractions. Analytical conditions in Table 1.

Fig. 7: On-line RPLC x SFC-qTOF separation of the full bio-oil sample: EIC 242.248 (green dotted line), 277.216 (red dotted line) and 284.295 (black dotted line). Analytical conditions in Table 1.

Fig. 8: Separation of a full bio-oil sample in (a) 1D-SFC with ACN/MeOH (50/50, v/v) as co-solvent (1 µL injected) and (b) on-line RPLC x SFC (3 µL injected): BPC (black) and EIC 172.170 (red). Other analytical conditions given in section 2.3.1. for 1D-SFC and in Table 1 for on-line RPLC x SFC.

Fig. 9: On-line RPLC x SFC-qTOF separation of (a, c) the full bio-oil and (b, d) the gasoline cut. Contour plots: BPC: (a, b); EIC 200.201 (c, d). Main differences are highlighted by the black dashed squares and the red dotted circles. Analytical conditions in Table 1.

Fig. S1. 1D-SFC base peak chromatogram of the gasoline cut using the Viridis BEH column (100x3.0 mm; 1.7 µm) and (a) methanol, (b) a mixture of acetonitrile and water (98/2) and (c) a mixture of acetonitrile and methanol (50/50) as co-solvent. Other analytical conditions: see section 2.3.1.

Fig. S2. Variation of the S as a function of log(k_0) for nine compounds in 1D-SFC with the ACN/H_2O (98/2, v/v) (orange) or ACN/MeOH (50/50) (blue) co-solvent.

Fig. S3. Three EICs in 1D-SFC using the BEH HILIC column (50x2.1 mm; 1.7 µm) and a mixture of acetonitrile and methanol (50/50) in (a) optimized 1D conditions (smooth gradient, see section 4.1.1.) and (b) the RPLC x SFC conditions (steep gradient, see Table 1). The dashed line corresponds to the determined RPLC x SFC limit showing the missing compounds beyond.

References

[1] J. Li, Z. Xiong, K. Zeng, D. Zhong, X. Zhang, W. Chen, A. Nzihou, G. Flamant, H. Yang, H. Chen, Characteristics and Evolution of Nitrogen in the Heavy Components of Algae Pyrolysis Bio-Oil, Environ. Sci. Technol. 55 (2021) 6373–6385. https://doi.org/10.1021/acs.est.1c00676.

[2] C.Y.B. Oliveira, A. Jacob, C. Nader, C.D.L. Oliveira, Â.P. Matos, E.S. Araújo, N. Shabnam, B. Ashok, A.O. Gálvez, An overview on microalgae as renewable resources for meeting sustainable development goals, J. Environ. Manage. 320 (2022) 115897. https://doi.org/10.1016/j.jenvman.2022.115897.

[3] M. Adamczyk, M. Sajdak, Pyrolysis Behaviours of Microalgae Nannochloropsis gaditana, Waste Biomass Valorization. 9 (2018) 2221–2235. https://doi.org/10.1007/s12649-017-9996-8.

[4] Z. Hu, X. Ma, C. Chen, A study on experimental characteristic of microwave-assisted pyrolysis of microalgae, Bioresour. Technol. 107 (2012) 487–493. https://doi.org/10.1016/j.biortech.2011.12.095.

[5] M.A. Rahman, Valorizing of weeds algae through the solar assisted pyrolysis: Effects of dependable parameters on yields and characterization of products, Renew. Energy. 147 (2020) 937–946. https://doi.org/10.1016/j.renene.2019.09.046.

[6] N. Neveux, A.K.L. Yuen, C. Jazrawi, M. Magnusson, B.S. Haynes, A.F. Masters, A. Montoya, N.A. Paul, T. Maschmeyer, R. de Nys, Biocrude yield and productivity from the hydrothermal liquefaction of marine and freshwater green macroalgae, Bioresour. Technol. 155 (2014) 334–341. https://doi.org/10.1016/j.biortech.2013.12.083.

[7] D. Xu, P.E. Savage, Characterization of biocrudes recovered with and without solvent after hydrothermal liquefaction of algae, Algal Res. 6 (2014) 1–7. https://doi.org/10.1016/j.algal.2014.08.007.

[8] Y. Xu, K. Liu, Y. Hu, Y. Dong, L. Yao, Experimental investigation and comparison of bio-oil from hybrid microalgae via super/subcritical liquefaction, Fuel. 279 (2020) 118412. https://doi.org/10.1016/j.fuel.2020.118412.

[9] B. Zhang, Z. He, H. Chen, S. Kandasamy, Z. Xu, X. Hu, H. Guo, Effect of acidic, neutral and alkaline conditions on product distribution and biocrude oil chemistry from hydrothermal liquefaction of microalgae, Bioresour. Technol. 270 (2018) 129–137. https://doi.org/10.1016/j.biortech.2018.08.129.

[10] L. Fan, H. Zhang, J. Li, Y. Wang, L. Leng, J. Li, Y. Yao, Q. Lu, W. Yuan, W. Zhou, Algal biorefinery to value-added products by using combined processes based on thermochemical conversion: A review, Algal Res. 47 (2020) 101819. https://doi.org/10.1016/j.algal.2020.101819.

[11] N. Sharma, K.K. Jaiswal, V. Kumar, M.S. Vlaskin, M. Nanda, I. Rautela, M.S. Tomar, W. Ahmad, Effect of catalyst and temperature on the quality and productivity of HTL bio-oil from microalgae: A review, Renew. Energy. 174 (2021) 810–822. https://doi.org/10.1016/j.renene.2021.04.147.

[12] D.L. Barreiro, W. Prins, F. Ronsse, W. Brilman, Hydrothermal liquefaction (HTL) of microalgae for biofuel production: State of the art review and future prospects, Biomass Bioenergy. 53 (2013) 113–127. https://doi.org/10.1016/j.biombioe.2012.12.029.

[13] M. Staš, J. Chudoba, D. Kubička, J. Blažek, M. Pospíšil, Petroleomic Characterization of Pyrolysis Bio-oils: A Review, Energy Fuels. 31 (2017) 10283–10299. https://doi.org/10.1021/acs.energyfuels.7b00826.

[14] Z. Tang, W. Chen, Y. Chen, J. Hu, H. Yang, H. Chen, Preparation of low-nitrogen and high-quality bio-oil from microalgae catalytic pyrolysis with zeolites and activated carbon, J. Anal. Appl. Pyrolysis. 159 (2021) 105182. https://doi.org/10.1016/j.jaap.2021.105182.

[15] D.F. Smith, D.C. Podgorski, R.P. Rodgers, G.T. Blakney, C.L. Hendrickson, 21 Tesla FT-ICR Mass Spectrometer for Ultrahigh-Resolution Analysis of Complex Organic Mixtures, Anal. Chem. 90 (2018) 2041–2047. https://doi.org/10.1021/acs.analchem.7b04159.

[16] P. Mikhaylova, L.P. de Oliveira, I. Merdrignac, A. Berlioz-Barbier, M. Nemri, P. Giusti, G.D. Pirngruber, Molecular analysis of nitrogen-containing compounds in vacuum gas oils hydrodenitrogenation by (ESI+/-)-FTICR-MS, Fuel. 323 (2022) 124302. https://doi.org/10.1016/j.fuel.2022.124302.

[17] R.V.S. Silva, N.S. Tessarolo, V.B. Pereira, V.L. Ximenes, F.L. Mendes, M.B.B. de Almeida, D.A. Azevedo, Quantification of real thermal, catalytic, and hydrodeoxygenated bio-oils via comprehensive two-dimensional gas chromatography with mass spectrometry, Talanta. 164 (2017) 626–635. https://doi.org/10.1016/j.talanta.2016.11.005.

[18] T. Schena, T.R. Bjerk, C. von Mühlen, E.B. Caramão, Influence of acquisition rate on performance of fast comprehensive two-dimensional gas chromatography coupled with time-of-flight mass spectrometry for coconut fiber bio-oil characterization, Talanta. 219 (2020) 121186. https://doi.org/10.1016/j.talanta.2020.121186.

[19] J. Crepier, A.L. Masle, N. Charon, F. Albrieux, P. Duchene, S. Heinisch, Ultra-high performance supercritical fluid chromatography hyphenated to atmospheric pressure chemical ionization high resolution mass spectrometry for the characterization of fast pyrolysis bio-oils, J. Chromatogr. B. 1086 (2018) 38–46. https://doi.org/10.1016/j.jchromb.2018.04.005.

[20] D. Guillarme, F. Rouvière, S. Heinisch, Theoretical and practical comparison of RPLC and RPLC × RPLC: how to consider dilution effects and sensitivity in addition to separation power?, Anal. Bioanal. Chem. (2022). https://doi.org/10.1007/s00216-022-04385-w.

[21] A.L. Masle, D. Angot, C. Gouin, A. D'Attoma, J. Ponthus, A. Quignard, S. Heinisch, Development of on-line comprehensive two-dimensional liquid chromatography method for the separation of biomass compounds, J. Chromatogr. A. 1340 (2014) 90–98. https://doi.org/10.1016/j.chroma.2014.03.020.

[22] E. Lazzari, K. Arena, E.B. Caramão, M. Herrero, Quantitative analysis of aqueous phases of bio-oils resulting from pyrolysis of different biomasses by two-dimensional comprehensive liquid chromatography, J. Chromatogr. A. 1602 (2019) 359–367. https://doi.org/10.1016/j.chroma.2019.06.016.

[23] E. Lazzari, K. Arena, E.B. Caramão, P. Dugo, L. Mondello, M. Herrero, Comprehensive two-dimensional liquid chromatography-based quali-quantitative screening of aqueous phases from pyrolysis bio-oils, ELECTROPHORESIS. 42 (2021) 58–67. https://doi.org/10.1002/elps.202000119.

[24] J. Crépier, E. Corbel, J.-M. Lerestif, A. Berthod, S. Heinisch, Characterization of positional isomers of drug intermediates by off-line RPLC x SFC hyphenated to high resolution MS, J. Pharm. Biomed. Anal. 202 (2021) 114142. https://doi.org/10.1016/j.jpba.2021.114142.

[25] H. Xin, Q. Fu, Y. Yuan, Y. Liu, Y. Ke, Y. Jin, X. Liang, Construction of an off-line two dimensional reversed-phase liquid chromatography/ultra-high performance supercritical fluid chromatography method for rapid and comprehensive analysis of Piper kadsura, J. Supercrit. Fluids. 127 (2017) 9–14. https://doi.org/10.1016/j.supflu.2017.03.004.

[26] W. Wei, J. Hou, C. Yao, Q. Bi, X. Wang, Z. Li, Q. Jin, M. Lei, Z. Feng, W. Wu, D. Guo, A high-efficiency strategy integrating offline two-dimensional separation and data post-processing with dereplication: Characterization of bufadienolides in Venenum Bufonis as a case study, J. Chromatogr. A. 1603 (2019) 179–189. https://doi.org/10.1016/j.chroma.2019.06.037.

[27] P.G. Stevenson, A. Tarafder, G. Guiochon, Comprehensive two-dimensional chromatography with coupling of reversed phase high performance liquid chromatography and supercritical fluid chromatography, J. Chromatogr. A. 1220 (2012) 175–178. https://doi.org/10.1016/j.chroma.2011.11.020.

[28] I. François, A. dos Santos Pereira, F. Lynen, P. Sandra, Construction of a new interface for comprehensive supercritical fluid chromatography×reversed phase liquid chromatography (SFC×RPLC), J. Sep. Sci. 31 (2008) 3473–3478. https://doi.org/10.1002/jssc.200800267.

[29] I. François, P. Sandra, Comprehensive supercritical fluid chromatography×reversed phase liquid chromatography for the analysis of the fatty acids in fish oil, J. Chromatogr. A. 1216 (2009) 4005–4012. https://doi.org/10.1016/j.chroma.2009.02.078.

[30] M. Sarrut, A. Corgier, G. Crétier, A.L. Masle, S. Dubant, S. Heinisch, Potential and limitations of on-line comprehensive reversed phase liquid chromatography×supercritical fluid chromatography for the separation of neutral compounds: An approach to separate an aqueous extract of bio-oil, J. Chromatogr. A. 1402 (2015) 124–133. https://doi.org/10.1016/j.chroma.2015.05.005.

[31] C. Barrère-Mangote, A. Roubaud, B. Bouyssiere, J. Maillard, J. Hertzog, J.L. Maître, M. Hubert-Roux, J.-F. Sassi, C. Afonso, P. Giusti, Study of Biocrudes Obtained via Hydrothermal Liquefaction (HTL) of Wild Alga Consortium under Different Conditions, Processes. 9 (2021). https://doi.org/10.3390/pr9091494.

[32] A. D'Attoma, C. Grivel, S. Heinisch, On-line comprehensive two-dimensional separations of charged compounds using reversed-phase high performance liquid chromatography and hydrophilic interaction chromatography. Part I: Orthogonality and practical peak capacity considerations, J. Chromatogr. A. 1262 (2012) 148–159. https://doi.org/10.1016/j.chroma.2012.09.028.

[33] D. Guillarme, V. Desfontaine, S. Heinisch, J.-L. Veuthey, What are the current solutions for interfacing supercritical fluid chromatography and mass spectrometry?, J. Chromatogr. B. 1083 (2018) 160–170. https://doi.org/10.1016/j.jchromb.2018.03.010.

[34] C. West, E. Lesellier, Effects of mobile phase composition on retention and selectivity in achiral supercritical fluid chromatography, J. Chromatogr. A. 1302 (2013) 152–162. https://doi.org/10.1016/j.chroma.2013.06.003.

[35] K. Plachká, T. Gazárková, J. Škop, D. Guillarme, F. Svec, L. Nováková, Fast Optimization of Supercritical Fluid Chromatography–Mass Spectrometry Interfacing Using Prediction Equations, Anal. Chem. 94 (2022) 4841–4849. https://doi.org/10.1021/acs.analchem.2c00154.

[36] T. Gazárková, K. Plachká, F. Svec, L. Nováková, Current state of supercritical fluid chromatography-mass spectrometry, TrAC Trends Anal. Chem. 149 (2022) 116544. https://doi.org/10.1016/j.trac.2022.116544.

[37] V. Desfontaine, A. Tarafder, J. Hill, J. Fairchild, A.G.-G. Perrenoud, J.-L. Veuthey, D. Guillarme, A systematic investigation of sample diluents in modern supercritical fluid chromatography, J. Chromatogr. A. 1511 (2017) 122–131. https://doi.org/10.1016/j.chroma.2017.06.075.

[38] M. Batteau, K. Faure, Effect of the injection of water-containing diluents on band broadening in analytical supercritical fluid chromatography, J. Chromatogr. A. 1673 (2022) 463056. https://doi.org/10.1016/j.chroma.2022.463056.

[39] R.D. Pauw, K. Shoykhet (Choikhet), G. Desmet, K. Broeckhoven, Understanding and diminishing the extra-column band broadening effects in supercritical fluid chromatography, J. Chromatogr. A. 1403 (2015) 132–137. https://doi.org/10.1016/j.chroma.2015.05.017.

[40] M. Enmark, D. Åsberg, A. Shalliker, J. Samuelsson, T. Fornstedt, A closer study of peak distortions in supercritical fluid chromatography as generated by the injection, J. Chromatogr. A. 1400 (2015) 131–139. https://doi.org/10.1016/j.chroma.2015.04.059.

[41] I. François, A. de Villiers, P. Sandra, Considerations on the possibilities and limitations of comprehensive normal phase–reversed phase liquid chromatography (NPLC×RPLC), J. Sep. Sci. 29 (2006) 492–498. https://doi.org/10.1002/jssc.200500451.

[42] J. Crepier, A.L. Masle, N. Charon, F. Albrieux, S. Heinisch, Development of a supercritical fluid chromatography method with ultraviolet and mass spectrometry detection for the characterization of biomass fast pyrolysis bio oils, J. Chromatogr. A. 1510 (2017) 73–81. https://doi.org/10.1016/j.chroma.2017.06.003.

Figure 1

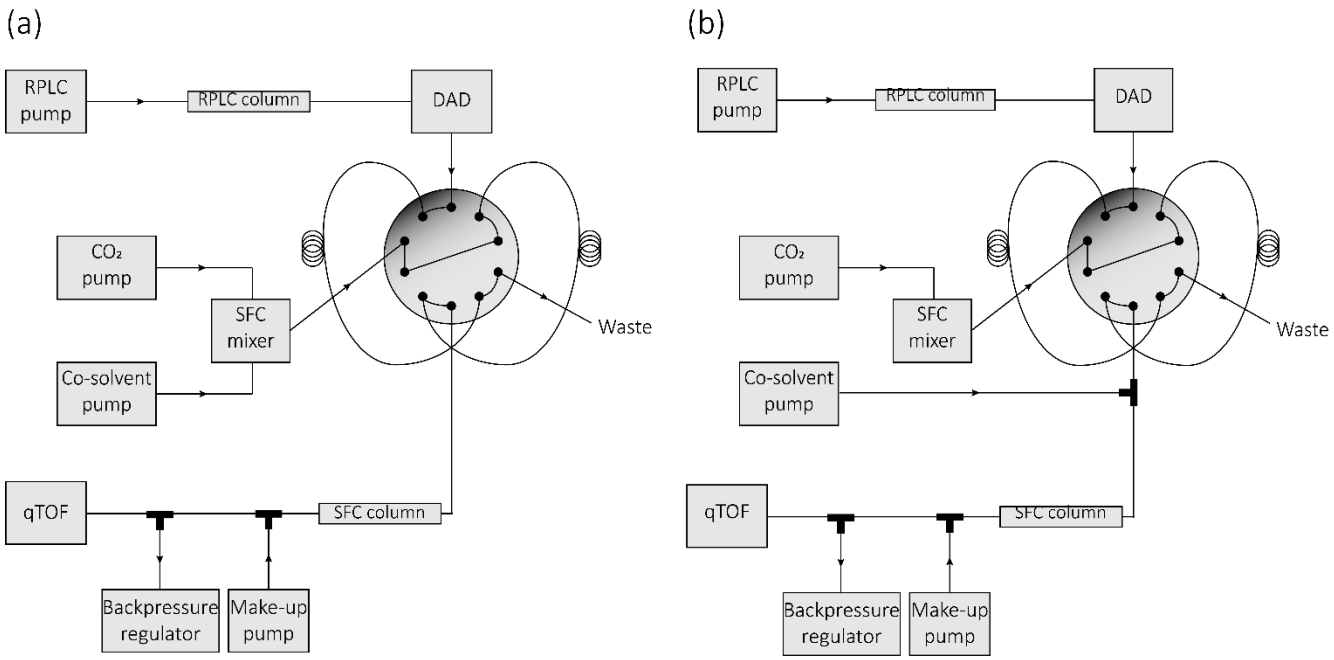
(a)
RPLC pump
RPLC column
DAD
CO₂ pump
SFC mixer
Co-solvent pump
Waste
qTOF
SFC column
Backpressure regulator
Make-up pump
(b)
RPLC pump
RPLC column
DAD
CO₂ pump
SFC mixer
Co-solvent pump
Waste
qTOF
SFC column
Backpressure regulator
Make-up pump

Figure 2

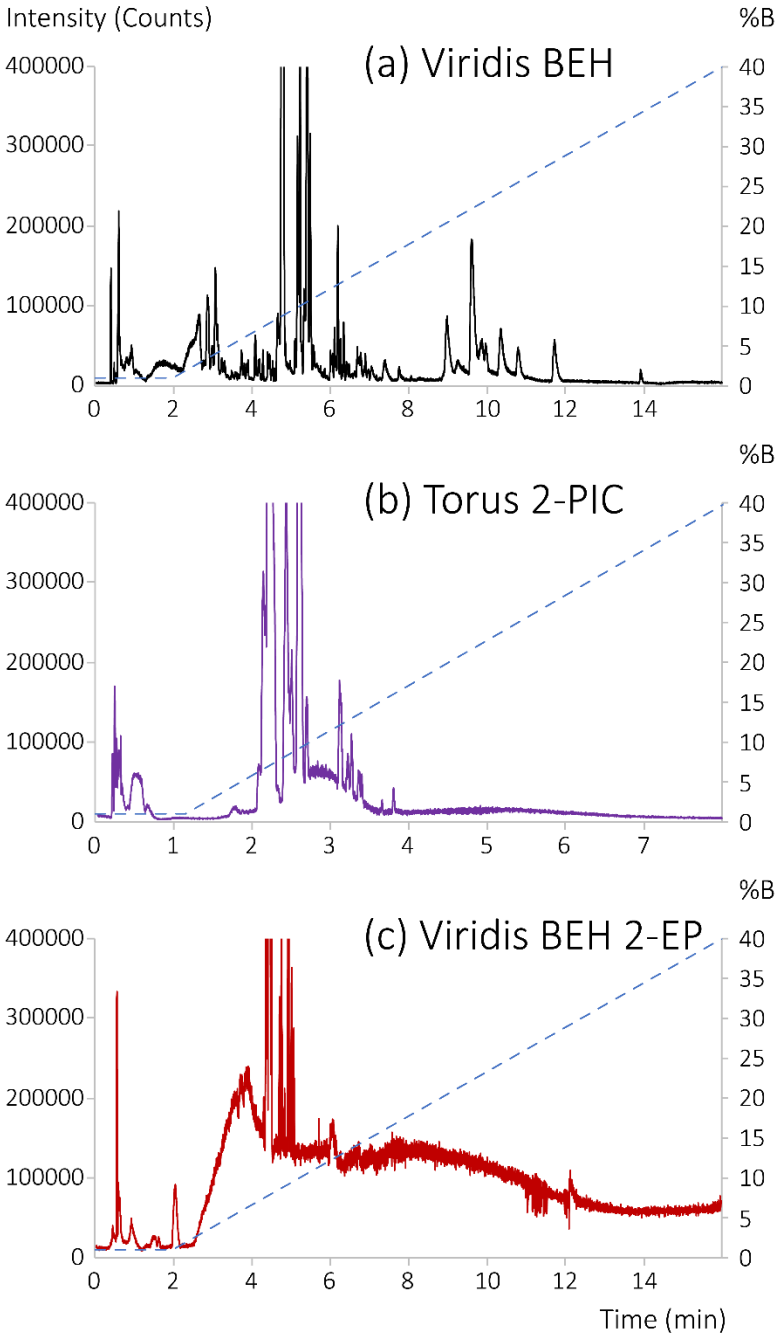
Intensity (Counts)
%B
(a) Viridis BEH
400000
300000
200000
100000
0
40
35
30
25
20
15
10
5
0
0 2 4 6 8 10 12 14
%B
(b) Torus 2-PIC
400000
300000
200000
100000
0
40
35
30
25
20
15
10
5
0
0 1 2 3 4 5 6 7
%B
(c) Viridis BEH 2-EP
400000
300000
200000
100000
0
40
35
30
25
20
15
10
5
0
0 2 4 6 8 10 12 14
Time (min)

Figure 3

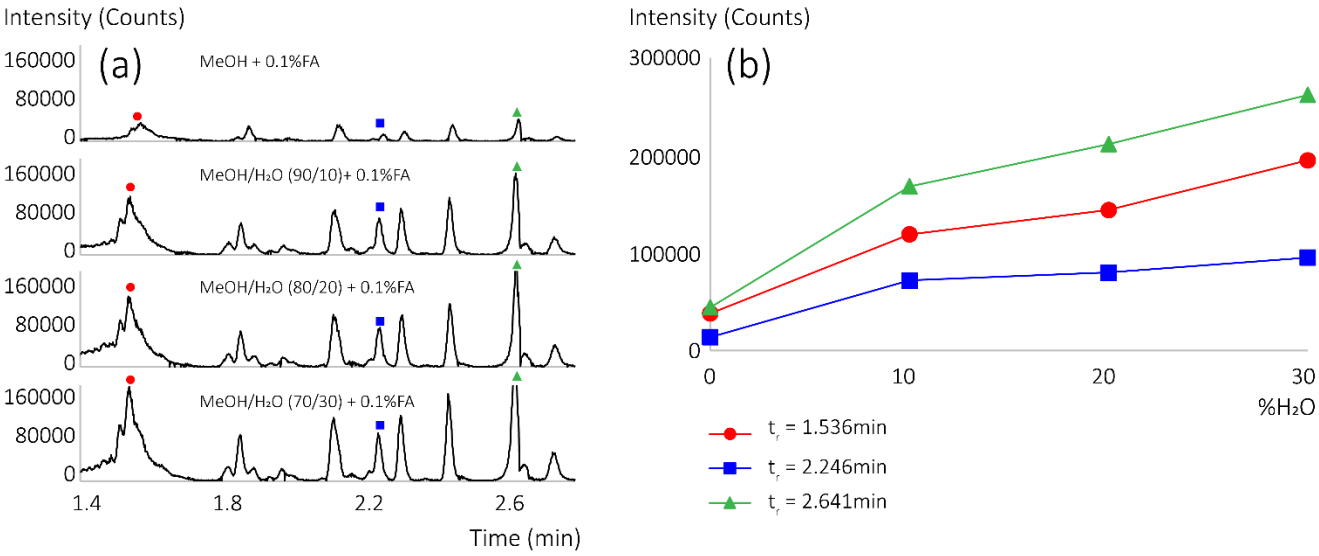
Intensity (Counts)
(a)
MeOH + 0.1%FA
MeOH/H₂O (90/10)+ 0.1%FA
MeOH/H₂O (80/20) + 0.1%FA
MeOH/H₂O (70/30) + 0.1%FA
160000
80000
0
1.4
1.8
2.2
2.6
Time (min)
Intensity (Counts)
(b)
300000
200000
100000
0
10
20
30
%H₂O
t_r = 1.536min
t_r = 2.246min
t_r = 2.641min

Figure 4

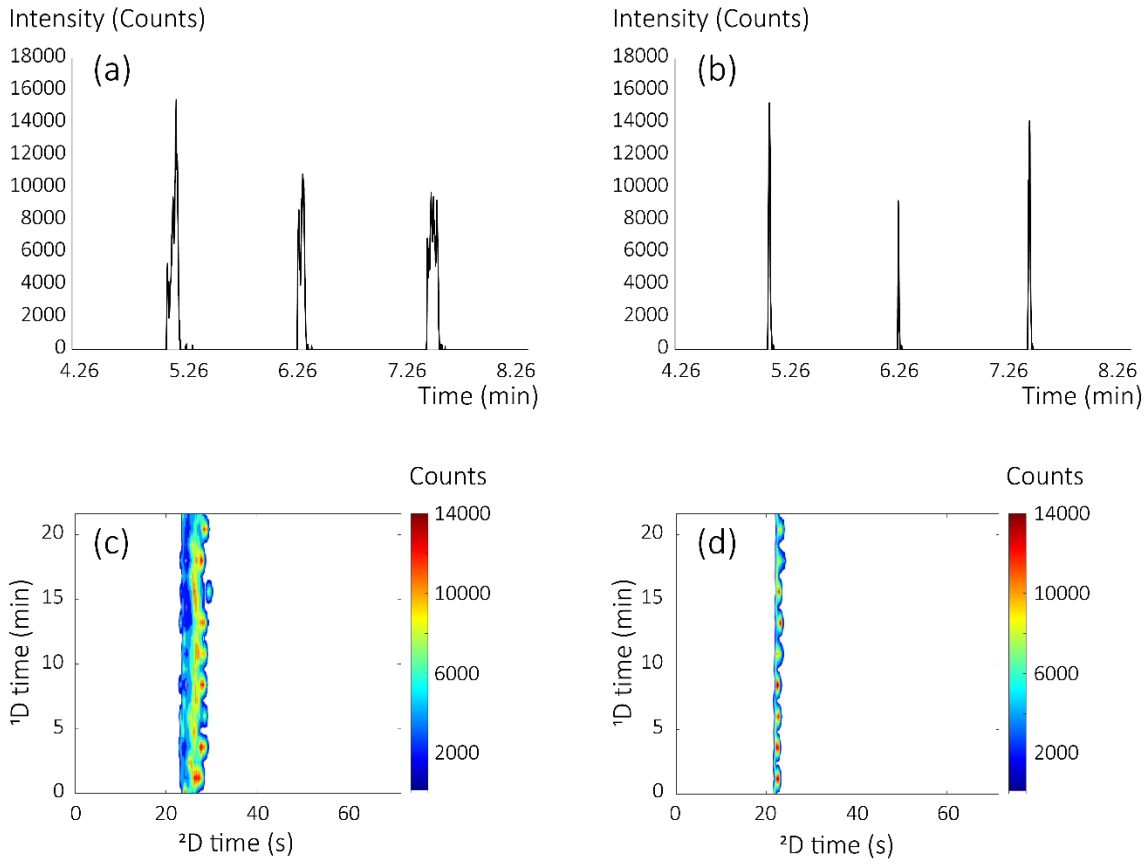
Intensity (Counts)
(a)
Time (min)
Intensity (Counts)
(b)
Time (min)
Counts
(c)
¹D time (min)
²D time (s)
Counts
(d)
¹D time (min)
²D time (s)

Figure 5

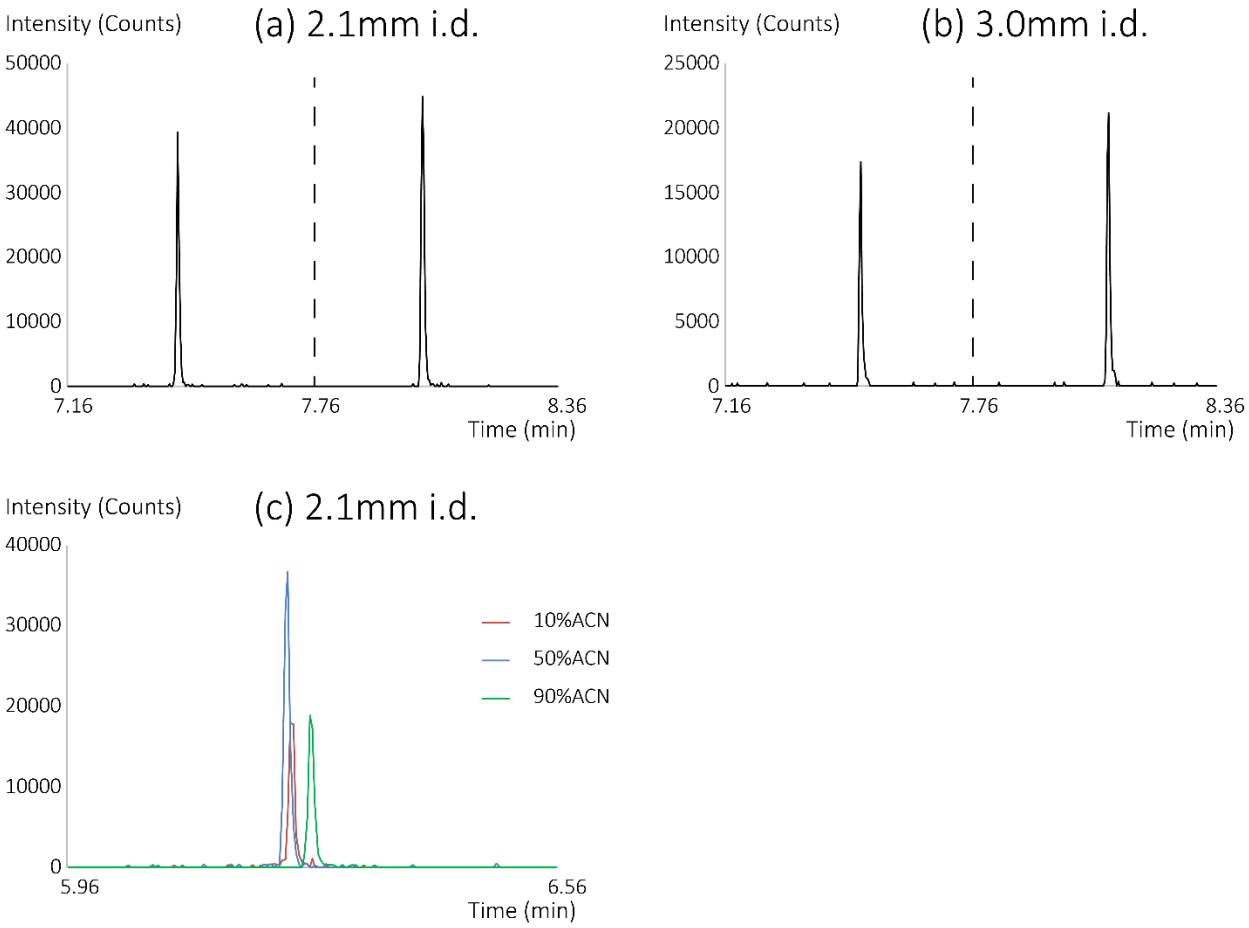
Intensity (Counts)
(a) 2.1mm i.d.
50000
40000
30000
20000
10000
0
7.16
7.76
8.36
Time (min)
Intensity (Counts)
(b) 3.0mm i.d.
25000
20000
15000
10000
5000
0
7.16
7.76
8.36
Time (min)
Intensity (Counts)
(c) 2.1mm i.d.
40000
30000
20000
10000
0
5.96
6.56
Time (min)
10%ACN
50%ACN
90%ACN

Figure 6

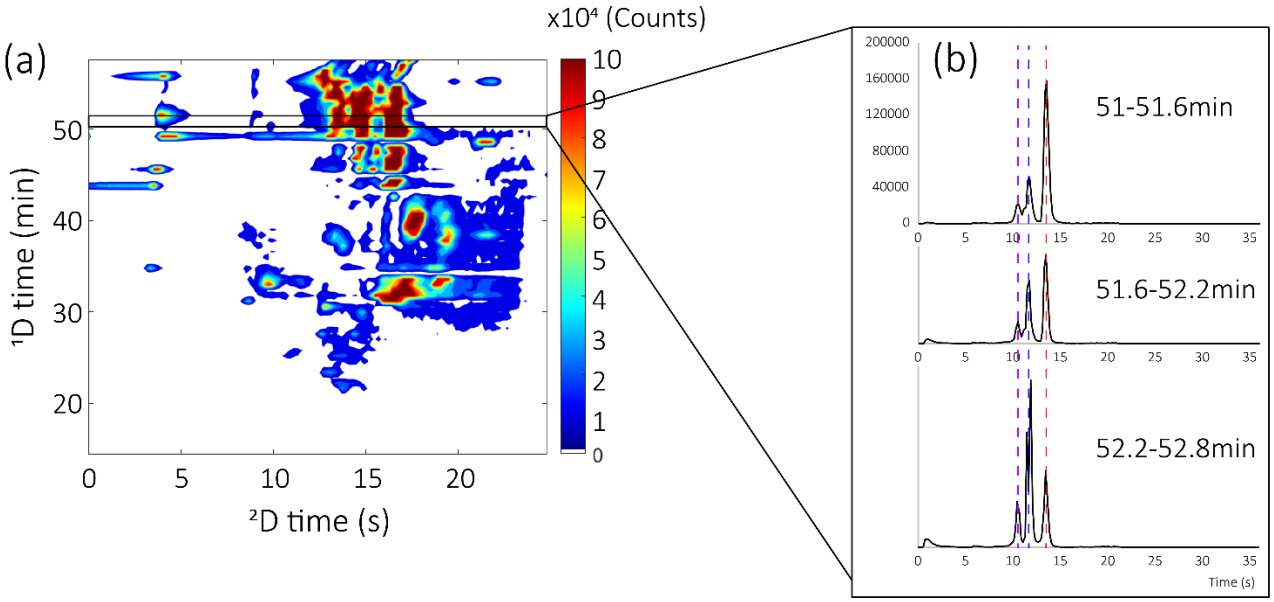
(a)
x10⁴ (Counts)
10
9
8
7
6
5
4
3
2
1
0
¹D time (min)
50
40
30
20
0
5
10
15
20
²D time (s)
(b)
200000
160000
120000
80000
40000
0
51-51.6min
51.6-52.2min
52.2-52.8min
0
5
10
15
20
25
30
35
Time (s)

Figure 7

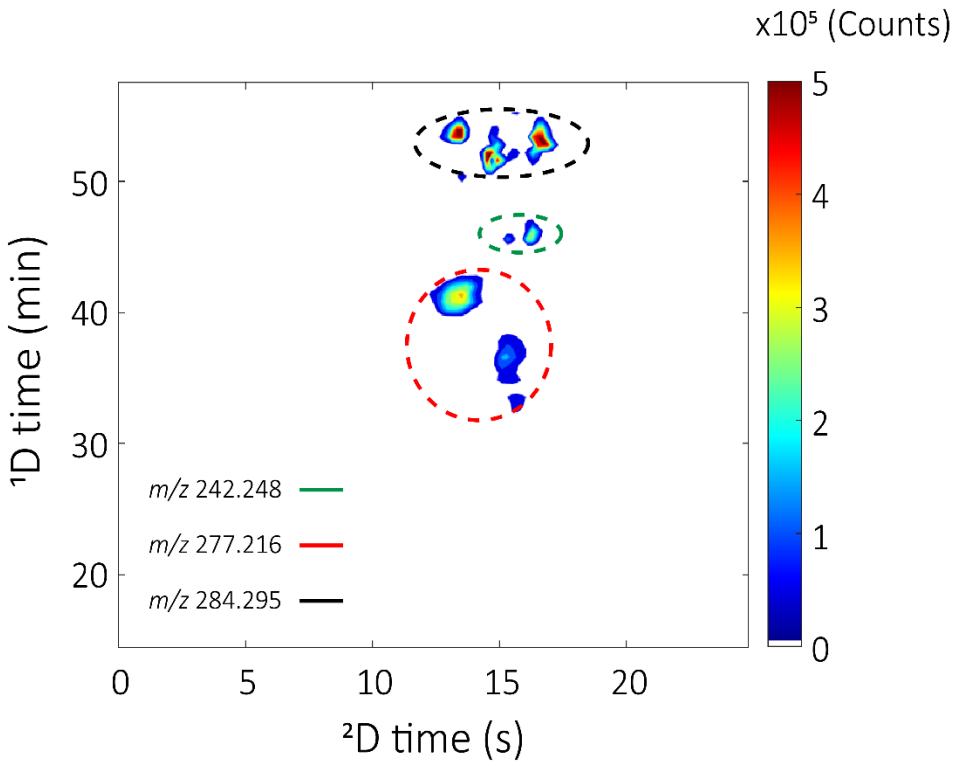
x10⁵ (Counts)
5
4
3
2
1
0
¹D time (min)
50
40
30
20
m/z 242.248
m/z 277.216
m/z 284.295
0
5
10
15
20
²D time (s)

Figure 8

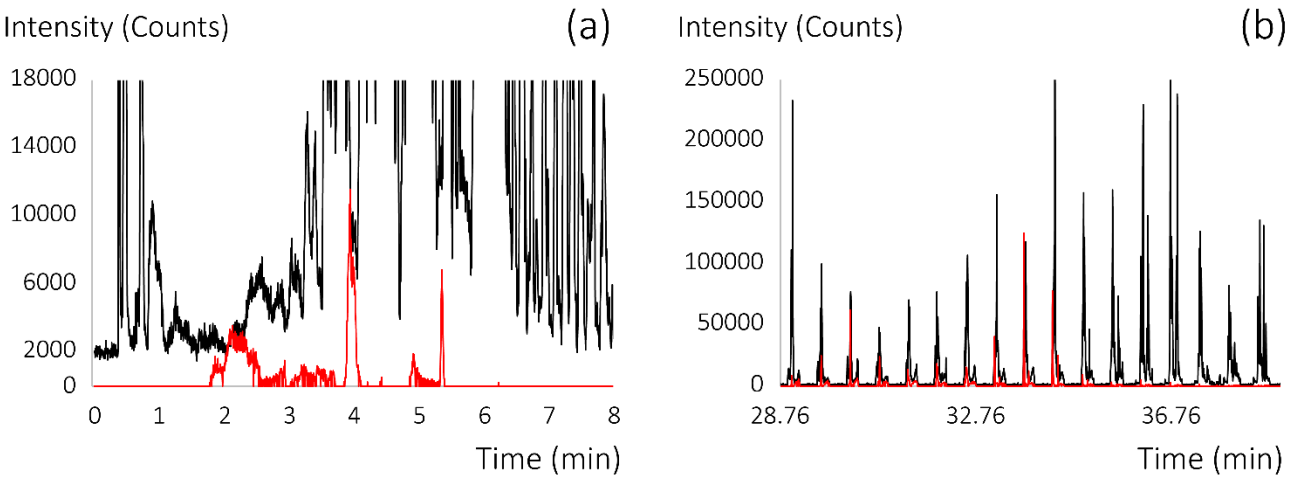
Intensity (Counts)
(a)
18000
14000
10000
6000
2000
0
0 1 2 3 4 5 6 7 8
Time (min)
Intensity (Counts)
(b)
250000
200000
150000
100000
50000
0
28.76
32.76
36.76
Time (min)

Figure 9

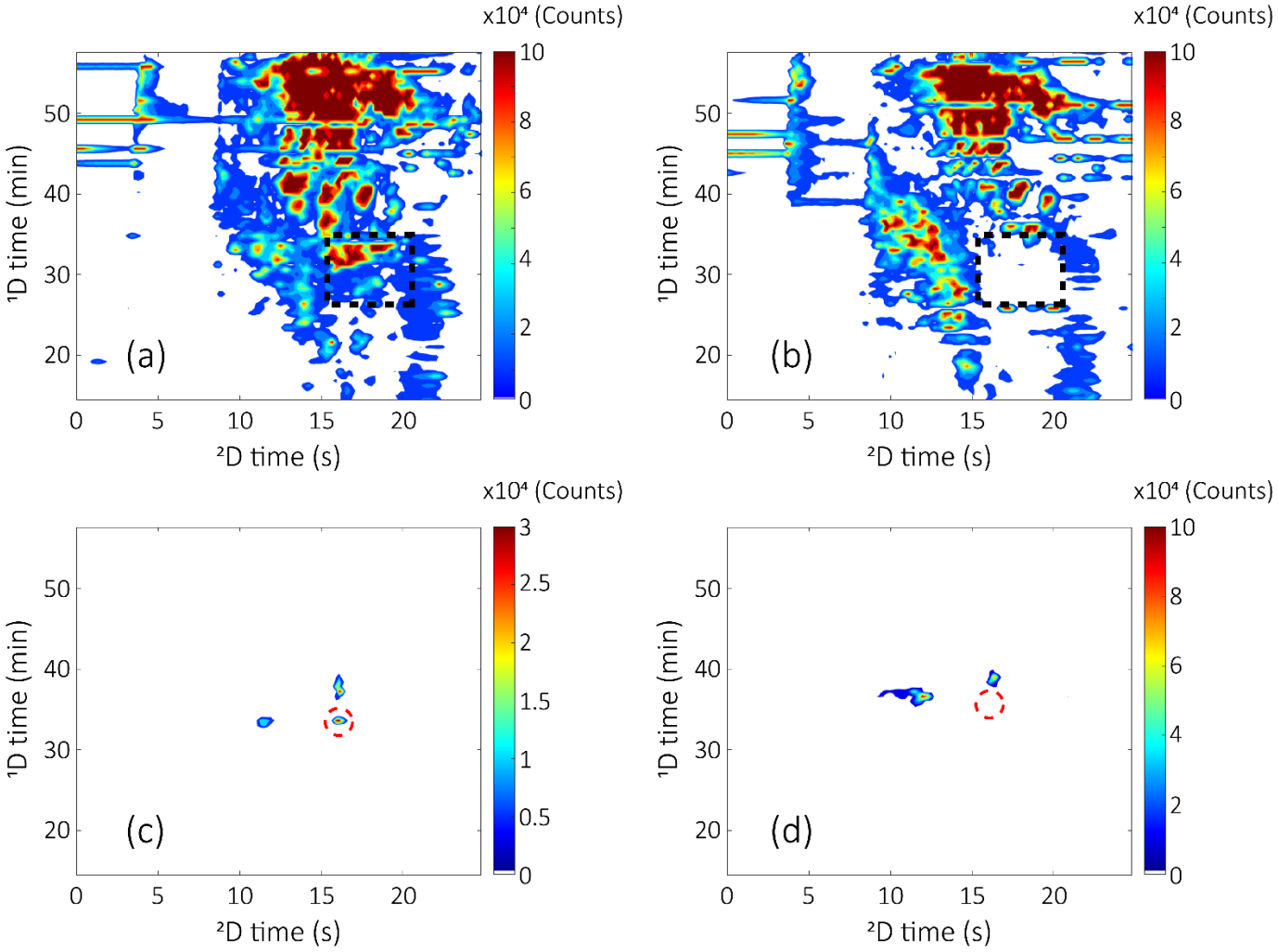

Table 1: Experimental conditions in on-line RPLC x SFC-qTOF

	^{1}D-RPLC	^{2}D-SFC
Column	XBridge BEH C18 (50x1.0mm; 3.5µm)	Acquity BEH HILIC (50x2.1mm; 1.7µm)
Injected volume (µL)	3	6
Flow rate (µL/min)	10	1800
Temperature (°C)	60	50
P_{BPR} (bar)	-	150
Mobile phase	A: H_2O, B: ACN	A: CO_2, B: ACN/MeOH (50/50, v/v)
Make-up solvent	-	MeOH/H_2O (90/10) +0.1%FA 500µL/min
Gradient elution	1-99%B in 45min	5-30%B in 0.25min, 30-5%B in 0.01min
Sampling time (min)	0.6	

Table 2: Comparison of elution composition range, peak capacity, and total pressure for three co-solvents with the Viridis BEH column (100x3.0mm, 1.7µm). See analytical conditions in section 2.3.1.

Co-solvent	Elution composition range (%)	Peak capacity	System pressure (bar) at 1.4mL/min
MeOH	27	186	355 at 40%B
ACN/H_2O (98/2, v/v)	41	195	360 at 60%B
ACN/MeOH (50/50, v/v)	29	193	350 at 40%B

Supplementary materials

Fig. S1. 1D-SFC base peak chromatogram of the gasoline cut using the Viridis BEH column (100x3.0mm; 1.7µm) and (a) methanol, (b) a mixture of acetonitrile and water (98/2) and (c) a mixture of acetonitrile and methanol (50/50) as co-solvent. Other analytical conditions: see section 2.3.1.

(a) B = MeOH

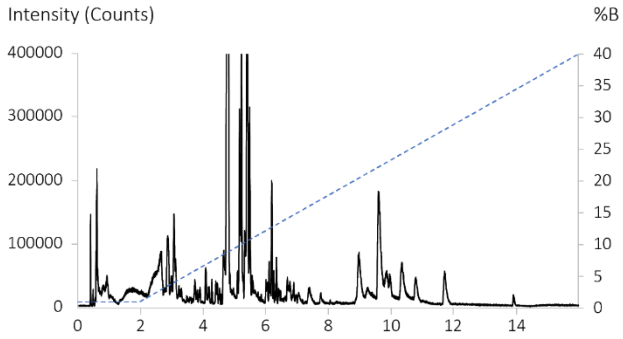

(b) B = ACN/H_2O (98/2, v/v)

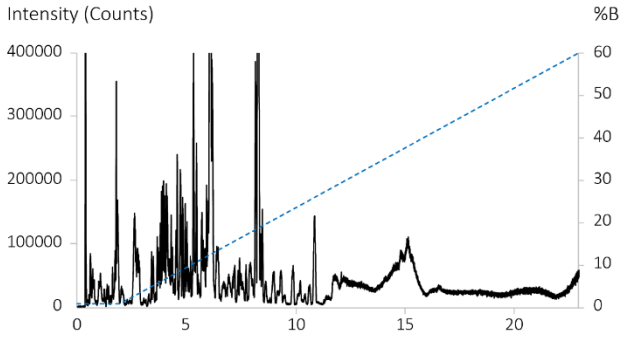

(c) B = ACN/MeOH (50/50, v/v)

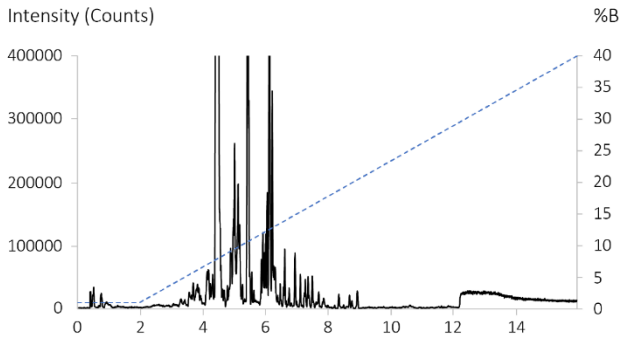

Fig. S2. Variation of S as a function of log(k_0) for nine compounds in 1D-SFC with the ACN/H_2O (98/2, v/v) (orange) or ACN/MeOH (50/50) (blue) co-solvent.

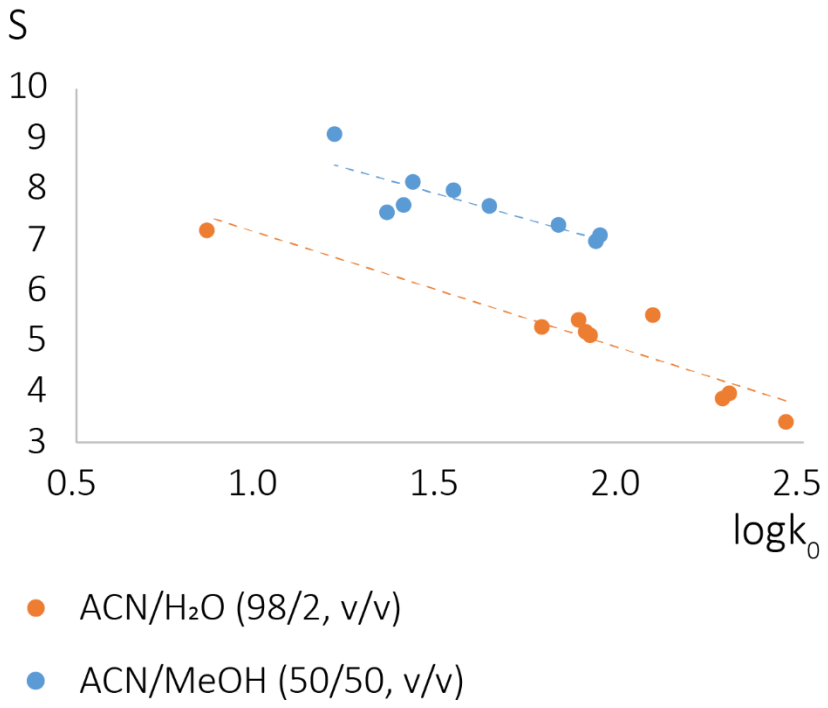

Fig. S3. Three EICs in 1D-SFC using the BEH HILIC column (50x2.1mm; 1.7µm) and a mixture of acetonitrile and methanol (50/50 v/v) in (a) optimized 1D conditions (smooth gradient, see section 4.1.1.) and (b) RPLC x SFC conditions (steep gradient, see Table 1). The dashed line corresponds to the determined RPLC x SFC limit showing the missing compounds beyond.

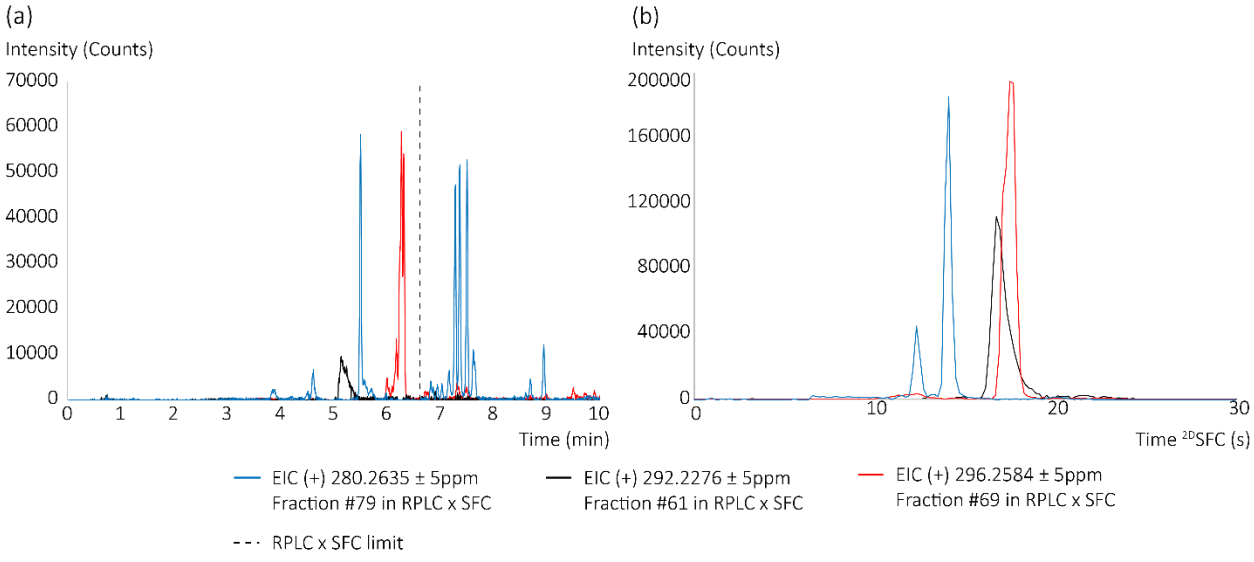

Table S1. Measured peak widths at 4σ (min) and resulting peak capacities for the six chromatographic systems studied.

	Chromatographic system					
m/z	Viridis BEH and ACN/H_2O	Viridis BEH and MeOH	Torus 2-PIC and ACN/H_2O	Torus 2-PIC and MeOH	Viridis BEH 2-EP and ACN/H_2O	Viridis BEH 2-EP and MeOH
278.248	0.088	0.060	0.114	0.051	0.114	0.051
280.264	0.087	0.056	0.133	0.095	0.216	0.095
284.295	0.082	0.085	-	0.070	0.095	0.070
263.237	0.095	0.053	0.107	0.075	0.105	0.075
256.264	0.094	0.041	0.133	0.100	0.104	0.058
228.233	0.082	0.043	0.155	0.116	0.099	-
296.258	0.085	0.092	0.104	0.112	0.117	0.061
298.311	0.051	-	0.070	-	0.095	0.054
Peak capacity (10cm column)	195	186	120	82	124	84

Table S2. Key parameters for peak capacity calculation in RPLC x SFC

Parameter	On-line RPLC x SFC
^{1}D RPLC peak capacity	51
^{2}D SFC peak capacity	22
γ	0.97
α	0.64
RPLC x SFC peak capacity	>700